

Electron–soliton dynamics in chains with cubic nonlinearity

M O Sales and F A B F de Moura

Instituto de Física, Universidade Federal de Alagoas, Maceió, AL 57072-970, Brazil

E-mail: fidelis@fis.ufal.br

Received 13 June 2014, revised 23 August 2014

Accepted for publication 29 August 2014

Published 23 September 2014

Abstract

In our work, we consider the problem of electronic transport mediated by coupling with solitonic elastic waves. We study the electronic transport in a 1D unharmonic lattice with a cubic interaction between nearest neighboring sites. The electron–lattice interaction was considered as a linear function of the distance between neighboring atoms in our study. We numerically solve the dynamics equations for the electron and lattice and compute the dynamics of an initially localized electronic wave-packet. Our results suggest that the solitonic waves that exist within this nonlinear lattice can control the electron dynamics along the chain. Moreover, we demonstrate that the existence of a mobile electron–soliton pair exhibits a counter-intuitive dependence with the value of the electron–lattice coupling.

Keywords: soliton, nonlinearity, electron

(Some figures may appear in colour only in the online journal)

1. Introduction

Lattice vibrations and their coupling with electronic dynamics (the electron–phonon interaction) play relevant roles in effective electronic transport [1–43]. In [8], the authors concluded that the superconducting state of *IrGe* is due to strong electron–phonon coupling. The authors in [9] also demonstrated that strong electron–phonon coupling is the mechanism behind the superconductivity of *La₂C₃*. Based on the *electrosoliton* concept proposed by Davydov and associated works, we know that the nonlinear character of the electron–lattice term can promote charge transport [19–43]. Davydov’s formalism consists of a Hamiltonian that describes the electronic dynamics under the influence of lattice vibrations. More recently, the existence of a *polaron–soliton* pair has been considered as a possible mechanism to promote charge transport [30–41]. This *polaron–soliton* ‘quasiparticle’ has been generally termed as a *solectron* [30–39]. It demonstrated the possibility of non-Ohmic supersonic electric conduction mediated by the *solectron* dynamics [38]. In [39], Velarde *et al* presented robust numerical evidence for the possibility of fast electron–soliton transport along the crystallographic axes of 2D unharmonic lattices. Moreover, the electronic dynamics in a Fermi–Pasta–Ulam disordered chain with electron–lattice interaction was considered in [42]. The electron–lattice

interaction was introduced by considering energy hopping as a function of the distance between neighboring atoms. By numerically solving the dynamics equations, evidence was found that the solitonic excitations induced by the nonlinear cubic interaction can control the electron dynamics along the entire lattice. The electron–soliton pair found in [42] was a direct consequence of the cubic nonlinearity of the α -Fermi–Pasta–Ulam model. We emphasize that in most works by Velarde *et al* (see [24–28, 30–38]), the electron–soliton pair was obtained by considering the nonlinear Morse potential. The possibility of electric conduction induced by nonlinear elasticity is a general issue with several connections to distinct fields of condensed matter. In [41], the electron transfer mediated by soliton-like excitations was investigated in several 2D anharmonic lattices, particularly in a square lattice similar to the cuprate lattice. The authors offered computational evidence of the possibility of almost loss-free electron–soliton transfer along the crystallographic axes. However, we emphasize that there is an open question about the existence and stability of thermal solitons (and solectrons) up to relatively high temperatures, e.g. room or physiological temperatures [38]. Recently, the problem of electron transfer in thermal lattices was investigated in [28, 33, 40]. These numerical calculations showed that the solectron-charge transport in the Toda–Morse lattice appears stable up to room temperature (about 300 K).

The main physical motivation behind the above topics is the identification of possible mechanisms of the charge transfer in DNA chains, polypeptides, bio molecules, and random lattices [43–50]. In [45], several theoretical models of charge transfer mechanisms in DNA models were discussed and the scopes of their application were analyzed. In particular, the authors focused on the charge transport induced by the polaron mechanism. The procedure considered in [45] is quite similar to that used by Velarde *et al*; the electronic dynamics was treated by a Quantum Hamiltonian and the lattice vibrations by a classical formalism. However, the electron-lattice interaction considered in [43, 45] was the standard SSH [51] approximation. Within the works of Velarde [24–28, 30–38], the electron-phonon term was introduced as an exponential of the distance between nearest neighbor atoms, which is a generalization of the linear SSH approximation. Moreover, the nonlinear term considered in [43, 45] was the cubic term, in contrast with the Toda–Morse potential considered by Velarde. The cubic potential used in [43, 45] represents an expansion of the Toda–Morse potential when the deviation from the equilibrium position is not very large [45].

In our work, we report further progress along these lines. We consider the problem of electron transport mediated by coupling with a solitonic wave. Our model consists of one electron moving in an unharmonic lattice and we focus on the existence of an electro–soliton pair similar to that obtained in [24–28, 30–43]. In our model, we consider a 1D unharmonic lattice with a cubic interaction between nearest neighboring sites. The electron–lattice interaction was introduced by considering the energy hopping following the SSH approximation, i.e. a linear function of the distance between neighboring atoms. We numerically solve the dynamics equations for the electron and lattice and compute the dynamics of an initially localized electronic wave-packet. Our results suggest that the solitonic waves that exist within this nonlinear lattice can control the electron dynamics along the entire lattice. We study in detail the formation of an electron–soliton state that can move along the chain. This mobile electron–soliton pair can be a key ingredient to the charge transport in a nonlinear chain. Moreover, we will investigate in detail the intensity of the electron-lattice interaction necessary to promote the appearance of this electron–soliton pair. Our calculations suggest that, even for strong electron-lattice coupling, we can find an electronic dynamics non-mediated by solitonic waves.

2. Model

In our model, we considered one electron moving in a chain of N masses. We considered that each mass is coupled with its nearest neighbors through a cubic force. We considered the electronic dynamics using a Quantum Hamiltonian and the lattice using a classical Hamiltonian. We also considered the coupling between the electron motion and atomic vibration. The electron-lattice interaction was considered by following the well-known SSH approximation. According to SSH theory, the electron’s kinetic energy depends on the effective distance between neighboring atoms. The complete Hamiltonian

for one electron coupled with the vibrations of a nonlinear chain can be written as $H = H_e + H_{\text{lattice}}$ where:

$$\begin{aligned} H_e &= \sum_n V_{n+1,n} (d_{n+1}^\dagger d_n + d_n^\dagger d_{n+1}) \\ H_{\text{lattice}} &= \sum_n h_n \end{aligned} \quad (1)$$

d_n^\dagger and d_n are the creation and annihilation operators for the electron at site n . $V_{n+1,n}$, representing the electron’s kinetic energy (the hopping term). $h_n(t)$ represents the classical energy of the n th-site and is defined by:

$$\begin{aligned} h_n &= \frac{P_n^2}{2m_n} + \frac{1}{4} [\beta_n (Q_{n+1} - Q_n)^2 + \beta_{n-1} (Q_n - Q_{n-1})^2] \\ &\quad + \frac{\eta}{6} [(Q_{n+1} - Q_n)^3 + (Q_n - Q_{n-1})^3] \end{aligned} \quad (2)$$

P_n and Q_n define the momentum and displacement of the mass at site (n), respectively. We considered all masses and elastic constants identical to $\beta_n = m_n = 1$. η represents the strength of the cubic non-linearity considered in our model. The classical Hamiltonian with cubic non-linearity considered here is the Fermi–Pasta–Ulam (FPU) α model [59]. The hopping elements $V_{n+1,n}$ depend on the relative distance between two consecutive molecules on the chain in the following the SSH expression:

$$V_{n+1,n} = -[V_0 - \alpha(Q_{n+1} - Q_n)] \quad (3)$$

V_0 is the transfer integral between the nearest-neighbor sites in the absence of electron-lattice coupling. α defines the effective electron-lattice coupling. In general, in the previous papers that have used the SSH approximation [1–7, 51], the parameter α was chosen $\alpha > V_0/a$ (a is the lattice parameter, in our work $a = 1$). Here, we follow this trend and consider $V_0 = 1$ and $\alpha > 1$. The time-dependent wave-function $|\Phi(t)\rangle = \sum_n c_n(t)|n\rangle$ was obtained by numerical solution of the time-dependent Schrödinger. We consider the electron initially localized at site $N/2$, i.e. $|\Phi(t=0)\rangle = \sum_n c_n(t=0)|n\rangle$ where $c_n(t=0) = \delta_{n,N/2}$. The Wannier amplitudes evolve in time according to the time-dependent Schrödinger equation as ($\hbar = 1$):

$$\begin{aligned} i \frac{dc_n(t)}{dt} &= -[1 - \alpha(Q_{n+1} - Q_n)]c_{n+1}(t) \\ &\quad - [1 - \alpha(Q_n - Q_{n-1})]c_{n-1}(t) \end{aligned} \quad (4)$$

Moreover, the lattice equation can be written as

$$\begin{aligned} \frac{d^2 Q_n(t)}{dt^2} &= (Q_{n+1} - Q_n) - (Q_n - Q_{n-1}) \\ &\quad + \eta[(Q_{n+1} - Q_n)^2 - (Q_n - Q_{n-1})^2] \\ &\quad - \alpha \{ (c_{n+1}^* c_n + c_{n+1} c_n^*) - (c_n^* c_{n-1} + c_n c_{n-1}^*) \} \end{aligned} \quad (5)$$

Our numerical formalism was based on the precise numerical solution of the previous equations (4) and (5). The dynamics equations for $c_n(t)$ and $Q_n(t)$ were solved by using a numerical method that consists of a combination of a high-order Taylor expansion [52] and a second order Euler procedure [53]. The electron dynamics equations (equation (4)) were solved

numerically using a high-order method based on the Taylor expansion of the evolution operator $U(\Delta t)$ [52]:

$$U(\Delta t) = \exp(-iH_e \Delta t) = 1 + \sum_{l=1}^{n_o} \frac{(-iH_e \Delta t)^l}{l!} \quad (6)$$

where H_e is the one-electron Hamiltonian. The wave-function at time Δt is given by $|\phi(\Delta t)\rangle = U(\Delta t)|\phi(t=0)\rangle$. The method can be used recursively to obtain the wave-function at time t . The classical equations (equation (5)) were solved using a second order Euler method defined as the following [53]: The procedure begins using a standard Euler method to find a prediction $Q_n(t + \Delta t)^*$ at the time $t + \Delta t$:

$$Q_n(t + \Delta t)^* \approx Q_n(t) + \Delta t \left. \frac{dQ_n}{dt} \right|_t \quad (7)$$

The next step consists of applying a correction formula in order to find an improved approximation to $Q_n(t + \Delta t)$

$$Q_n(t + \Delta t) \approx Q_n(t) + \frac{\Delta t}{2} \left[\left. \frac{dQ_n}{dt} \right|_t + \left. \frac{dQ_n^*}{dt} \right|_{t+\Delta t} \right] \quad (8)$$

The following results were obtained using $\Delta t = 10^{-3}$ and the sum of equation (6) was truncated at $n_o = 10$. This procedure was sufficient to keep the wave-function norm conservation along the entire time interval considered ($|1 - \sum_n |c_n(t)|^2| < 10^{-8}$). We emphasize that, in order to ensure accuracy of our compost numerical procedure, we compared our calculations with the results obtained using the standard fourth-order Runge–Kutta (RK4) [53]. The results obtained with our numerical formalism are in excellent agreement with (RK4). Moreover, our formalism requires a computational time lower than in the case of (RK4).

Aiming to characterize the dynamic behavior of the wave packet, we computed a typical quantity that can describe the electronic transport in this nonlinear model, namely the participation function defined as [54, 55]

$$\xi(t) = 1 / \sum_n |c_n(t)|^4. \quad (9)$$

The participation function provides an estimate of the number of base states over which the wave packet is spread at time t . In particular, the asymptotic participation number becomes size-independent for localized wave packets. On the other hand, $\xi(t \rightarrow \infty) \propto N$ corresponds to the regime where the wave packet is uniformly distributed over the lattice [54, 55].

3. Results

In our calculations, we followed the time evolution of a wave-packet initially localized at the center of a self-expanding chain. The self-expanding chain was used to avoid boundary effect; whenever the probability of finding the particle at the ends of the chain exceeded 10^{-30} , twenty new sites were added to each end. The initial wave-packet is defined as $\{c_n(t=0) = \delta_{n,n_0}\}$ where n_0 represents the center of the self-expanding chain. A high-order method based on the Taylor expansion of the evolution operator was used to solve the set of

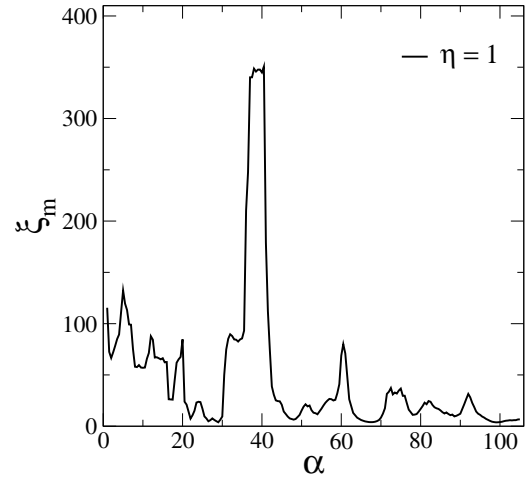


Figure 1. The long-time participation function ($\xi_m = \lim_{t \rightarrow t_{\max}} \xi(t)$) versus the electron-lattice coupling strength α . t_{\max} was considered about 2×10^4 units and the strength of the cubic and harmonic forces $\eta = \beta = 1$.

time-dependent Schrödinger coupled equations (equation (4)) and the second-order Euler method to solve the classical lattice equations (equation (5)). The lattice equations were solved by considering an initial energy input fully localized at the center n_0 of the self-expanding chain, i.e. $\{Q_n(t=0) = 0\}$ and $\{\dot{Q}_n(t=0) = \delta_{n,n_0}\}$. Numerical convergence was ensured by checking the conservation of the norm of the wave-packet at each time step. In our calculations, $|1 - \sum_n |c_n(t)|^2| < 10^{-8}$ along the entire time considered. Figure 1 shows the long-time limit of the participation function $\xi_m = \lim_{t \rightarrow t_{\max}} \xi(t)$ versus the electron-lattice coupling strength α . In our calculations, t_{\max} was considered as about 2×10^4 units. Calculations were performed considering the strength of the cubic and harmonic forces $\eta = \beta = 1$. Figure 1 shows the existence of certain regions with a large participation number and other regions in which the participation number ξ_m is less than 10 sites (some valleys). Therefore, our results suggest that, depending on the α value chosen, the electronic wave-packet can become extremely localized or exhibit some spread along the lattice. This result deserves more detailed analysis. The first point of our analysis focuses on understanding what is happening with the electronic wave-packet in both regimes. We focused on the time-dependent participation number $\xi(t)$ versus time t for several values of the electron-lattice coupling α (see figures 2(a) and (b)). We tuned the values of α to investigate both the case with the larger participation number ($\alpha = 5, 19, 32, 37$) as well as the case in which the wave-packet remains localized ($\alpha = 27.5, 47.5, 67.5, 100$). We observe in figure 2(a) that the participation number for $\alpha = 5, 19, 32, 37$ increases with time t approximately as $\xi \propto t^{0.25(3)}$. In [12, 15, 17], the electronic dynamics in a nonlinear Schrödinger equation was investigated and a similar sub-diffusive propagation was also observed. We emphasize that the effective nonlinearity considered in [12, 15, 17] was raised from the interaction with the lattice phonons. Moreover, our results in figure 2(a) are in good agreement with the results shown in figure 1 for the same values of α . However, the results in figure 2(b) show that, for short-times, the

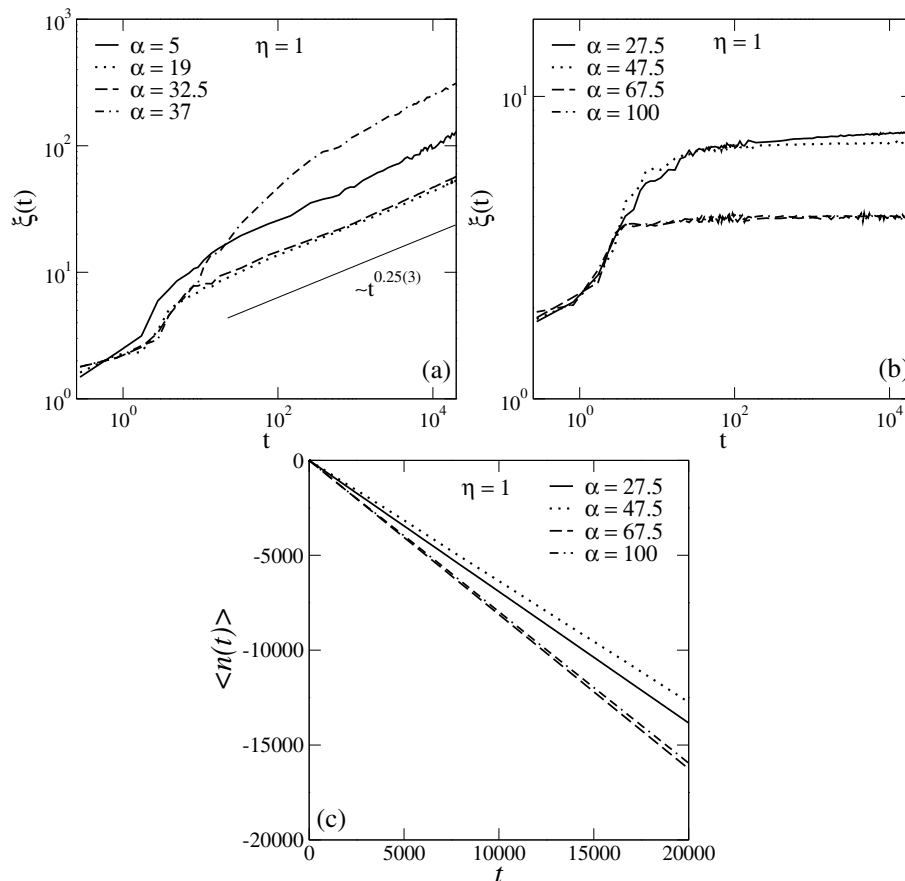


Figure 2. (a, b) Time-dependent participation number $\xi(t)$ versus time t for several values of the electron-lattice coupling α . (a) The case with larger participation number ($\alpha = 5, 32.5, 37.5, 60$); (b) the case in which that the wave-packet remains fully localized ($\alpha = 27.5, 47.5, 67.5, 100$); and (c) the mean position of the wave-packet $\langle n(t) \rangle$ for the fully localized regime with $\alpha = 27.5, 47.5, 67.5, 100$. $\langle n(t) \rangle = 0$ represents the center of the chain, i.e. the initial position.

participation number for $\alpha = 27.5, 47.5, 67.5, 100$ increases until there are few sites (less than 10) saturated for long-times. The saturation of ξ at the long-time limit is in perfect agreement with the calculations of the participation number found at the valleys of figure 1. In figure 2(c), we focused on the electronic mobility for those cases in which the nonlinear coupling α is chosen within the valleys of the figure 1. We computed the time evolution of the mean position (centroid) defined as [54, 55] $\langle n(t) \rangle = \sum_n n |c_n(t)|^2$ for $\alpha = 27.5, 47.5, 67.5, 100$. We emphasize that for these values of α the wave-packet remains localized for long-times. We can see that, in spite of the width of wave-function remaining finite (see figure 2(a)), the wave-packet centroid evolves along time. This result suggests that this localized electronic wave-packet has mobility and thus charge transport is possible within this nonlinear chain.

Therefore, our results shown in figures 2(a) and (c) demonstrate that the electron wave-function can become trapped in a small fraction of the chain. We now investigate some specificities of this fully localized behavior. We examine the time-dependent wave-function profile. In figures 3(a)–(d), we plot $|c_n|^2$ versus t and n for $\eta = \beta = 1$ and $\alpha = 27.5, 47.5, 67.5, 100$ (we chose distinct values of α in which the electron wave-function remains fully localized).

Calculations were performed in a finite lattice with $N = 600$ sites. It is clearly in good agreement with results shown in figures 1 and 2. The wave-function remains trapped in a finite fraction of the lattice. We can also see that the localized electronic wave-packet is moving along the chain. The mobility found in figure 3 is in good agreement with the centroid calculations shown in figure 2(c). It should be noted that we are dealing with an unharmonic chain with cubic nonlinearity. Therefore, the nonlinear interaction between the nearest neighbor atoms promotes the appearance of a soliton mode [56–60]. The dynamics of this soliton mode is directly related to the type of nonlinearity considered and the type of initial condition chosen. For example, within the present model with cubic nonlinear forces, the direction of the motion can be inverted by exchanging the sign of the initial velocity excitation. figure 4 shows the spatial and temporal evolution of the lattice deformation $A_n = \exp[(Q_n - Q_{n-1})]$ and the energy $h_n(t)$ of the mass at site (n). We plot A_n and $h_n(t)$ times t and n for the anharmonic chain with $\eta = 1$ and the electron-phonon coupling $\alpha = 27.5$. Our results show that the initial excitation propagates along the classical chain in a solitonic state. We observed that the lattice deformation A_n moves in an invariant form with constant velocity over the chain. Moreover,

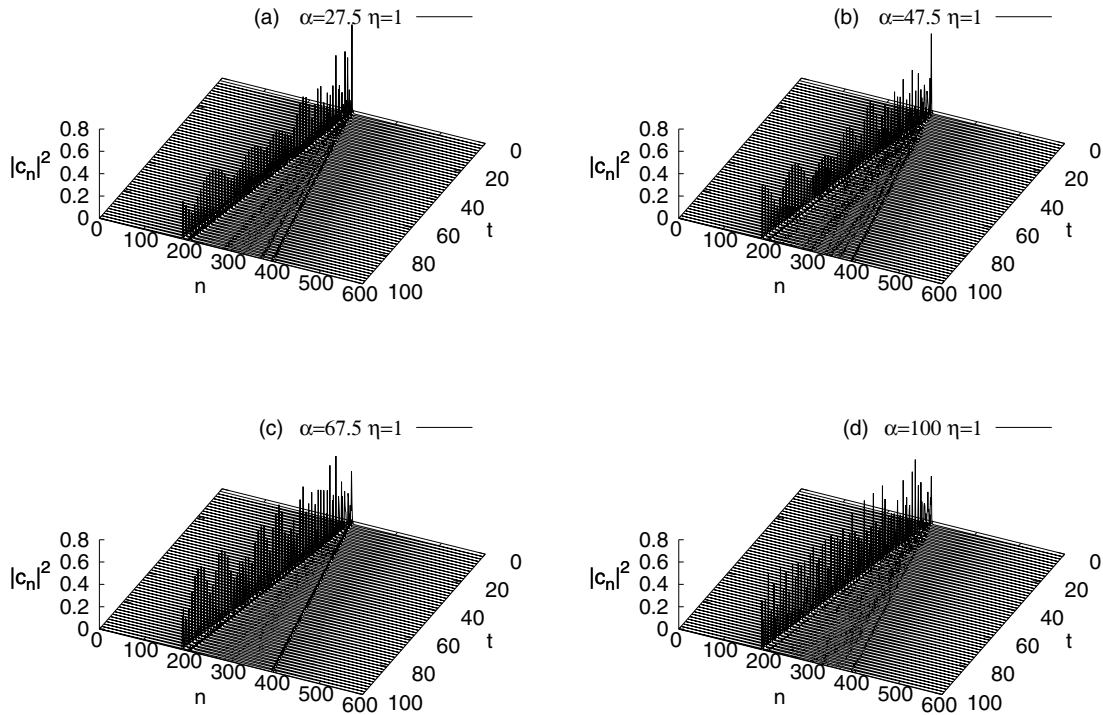


Figure 3. The wave-function component $|c_n|^2$ versus t and n for $\eta = \beta = 1$ and $\alpha = 27.5, 47.5, 67.5, 100$. The majority of the initial wave-packet is trapped by the solitonic wave and this electron-soliton pair exhibits mobility along the chain.

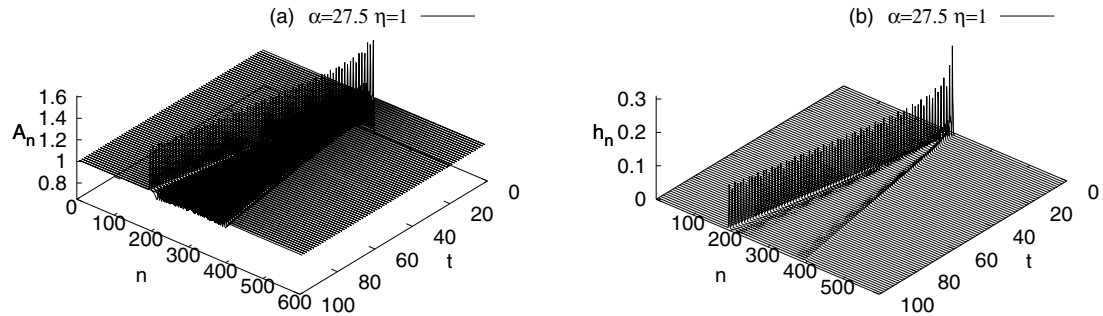


Figure 4. The lattice deformation $A_n = \exp[(Q_n - Q_{n-1})]$ and the local energy $h_n(t)$ versus t and n for an anharmonic chain with cubic nonlinearity $\eta = 1$ and electron-lattice coupling $\alpha = 27.5$. Our results show that the initial excitation propagates along the chain in a solitonic state.

we also observed that the energy intensity of this soliton-like mode appears to remain constant and moving along the lattice. The energy pulse profile shown in figures 4(a) and (b) is a clear signature of the presence of a solitonic mode within the nonlinear harmonic lattice. Therefore, the results shown in figure 4 are in good agreement with the wave-function dynamics obtained in figures 3(a-d) thus supporting the hypothesis of the electron-soliton pair formation. Therefore, our calculations suggest that the electron-lattice interaction considered here promotes the appearance of a mobile electron-soliton pair. The electron-soliton excitation observed here is quite similar to those obtained in [30–42]. We observed that the soliton mode can trap most part of the initial electronic wave-packet. The dynamics of this electron-soliton pair seem to be dominated by the mobility of the solitonic mode [30–39].

We also investigated the wave-function spatial profile at the cases in which the participation number increases with time. The spatial profile of the wave-function fully fills the (t, n) plane. Therefore, a three dimensional presentation using $(|c_n(t)|^2, t, n)$ does not provide a good visualization of the data in this case. Therefore, we plotted in figure 5 $|c_n(t)|^2$ versus n for several instants and electron-phonon coupling α . We tuned α to choose the cases in which the participation number increases with time t . We are interested in analyzing the electronic dynamics in those cases with apparent absence of the electron-soliton pair. We performed our calculations in a finite chain with $N = 2000$ sites. We considered $\eta = \beta = 1$, $\alpha = 37, 60$ and $t = 200, 400, 600, 800$. We again emphasize again that for these values of α , the participation number increases with time t and, therefore, the electron-soliton pair apparently does not exist. We observed

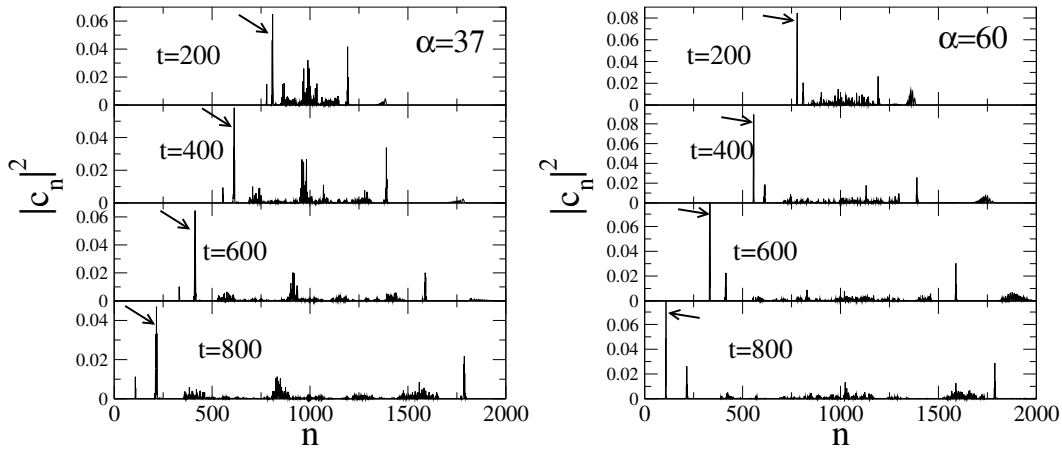


Figure 5. $|c_n(t)|^2$ versus n for several instants and electron-lattice couplings α . Calculations were performed for $\alpha = 37, 60$. For these cases the participation number is increased with time t and the electron–soliton pair apparently does not exist.

that the wave-packet spreads along the entire lattice in good agreement with the behavior of the participation number found in figure 2(a). However, we observed that even from the initial stage, the wave packet splits in a structure with two peaks that move in opposite directions. Particularly, we observed that one of these peaks (the peak at the left of the center of the chain) keeps its intensity approximately constant along time (see the arrows). Usually, within the context of time-dependent electronic dynamics, the initial wave packet should split from its single peak structure to a structure with two stable peaks that move in opposite directions [61]. Moreover, from [61], we know that these two peaks should exhibit a small finite width and that this width increases as time is increased. In our study, the one-electron dynamics displays behavior somewhat different from the standard theory [61]. The peak structure reported in figure 5 exhibits some similarities with the one-electron wave-packet profile found in [13]. Our results suggest that, in spite of the wave-packet spreading along the chain, we can find some elements associated with the formation of electron–soliton pair. The mobile peaks found (see the arrows in figure 5) suggest that a small finite fraction of the initial wave-packet is trapped by the solitonic modes. However, most of the wave-packet is decoupled of the solitonic mode and propagates along the chain. Therefore, we have found some evidence that suggests that even in the case where the electron–phonon coupling α is tuning on the peaks of figure 1, a small fraction of the wave-packet is trapped by the solitonic waves. However, the electron–phonon interaction at these cases is not sufficient to dominate the electronic dynamics.

4. Summary

In our work, we studied the dynamics of a one-electron in a unharmonic chain at the presence of the electron-lattice interaction. We considered a Fermi–Pasta–Ulam lattice with a cubic potential. The electron transport was treated by following a quantum tight-binding approximation and the longitudinal vibrations of the lattice were described using a classical formalism. The interaction between the electron and the lattice

was considered such that the transfer integral between neighboring atoms was dependent on the effective distance between neighboring atoms. We used the SSH approximation, meaning that the hopping term is defined as a linear function of the distance between neighboring atoms. By using a high precision procedure for solving the dynamics equations for the electron and lattice, we computed the spreading of an initially localized one-electron wave-packet. Our results suggest that the soliton mode that exists within this nonlinear lattice can control the electron dynamics along the entire lattice. Our data revealed a kind of electron–soliton state moving along the chain. This mobile electron–soliton pair exhibits a velocity approximately constant and can be a key ingredient in the charge transport in a nonlinear chain. These results are in good agreements with recent works [24–28, 30–38, 42] that point out the existence of a new excitation resulting from the trapping of an electron by a solitonic wave. Moreover, we demonstrated the range of α values necessary to promote the appearance of this electron–soliton pair. Our calculations suggest that, even for strong electron-lattice coupling α , we can determine the absence of electron–soliton dynamics. This is a non-intuitive result. In general, we would expect that as the electron-lattice coupling α is increased, it should be easier to promote electron trapping and, consequently, electron–soliton pair formation. However, within the cubic nonlinearity considered in our work, our results suggest that this is not true. We emphasize that our calculations were performed in a Fermi–Pasta–Ulam lattice with a cubic potential and the electron-lattice term was considered by following the SSH approximation. We also stress that a direct comparison with the results of Velarde is difficult. Velarde *et al* obtained the electron–soliton pair by considering the orse potential and the hopping term following an exponential of the distance between nearest atoms. The cubic potential in the SSH approximation considered here are properties similar to the Velarde approach at the limit of weak vibrations. Therefore, we suspect that the behavior reported in our paper should also appear within the approach they used. Moreover, we also emphasize that we did not consider the difference τ between the time scale of the electron dynamics and the time scale of

the lattice vibrations. Velarde *et al* used an artifice of to multiply the right side of the quantum Schrödinger equation by τ in order to include the difference between both time scales. We stress that this procedure represents an increase of the electronic hopping intensity and promotes only a rescaling of the electron-lattice coupling range of values. We hope that our paper can stimulate discussion along this line.

Acknowledgments

This work was partially supported by CNPq, CAPES, and FINEP (Federal Brazilian Agencies), and CNPq-Rede Nanobioestruturas, as well as FAPEAL (Alagoas State Agency). The research work of M O Sales is supported by a graduate program of CAPES.

References

- [1] Teramoto T, Wang Z, Kobryanskii V M, Taneichi T and Kobayashi T 2009 *Phys. Status Solidi* **6** 311–4
- [2] Wei J H, Wang L X, Chan K S and Yan Y J 2005 *Phys. Rev. B* **72** 064304
- [3] Conwell E M and Rakhmanova S V 2000 *Proc. Natl Acad. Sci. USA* **97** 4556–60
- [4] Li M and Lin X 2010 *Phys. Rev. B* **82** 155141
- [5] Vos F L J, Aalberts D P and van Saarloos W 1996 *Phys. Rev. B* **53** 14922
- [6] de Oliveira Neto P H, da Cunha W F and Silva G M e 2009 *Europhys. Lett.* **88** 67006
- [7] Marchand D J J, De Filippis G, Cataudella V, Berciu M, Nagaosa N, Prokof'ev N V, Mishchenko A S and Stamp P C E 2010 *Phys. Rev. Lett.* **105** 266605
- [8] Hirai D, Ali M N and Cava R J 2013 *J. Phys. Soc. Japan* **82** 124701
- [9] Kim J S *et al* 2007 *Phys. Rev. B* **76** 014516
- [10] Kopidakis G, Soukoulis C M and Economou E N 1996 *Europhys. Lett.* **33** 459
- [11] Kopidakis G and Soukoulis C M 1995 *Phys. Rev. B* **51** 15038
- [12] Ivanchenko M V 2009 *Phys. Rev. Lett.* **102** 175507
- Flach S, Krimer D O and Skokos C H 2009 *Phys. Rev. Lett.* **102** 024101
- Skokos C H, Krimer D O, Komineas S and Flach S 2009 *Phys. Rev. E* **79** 056211
- Sangiovanni G, Capone M, Castellani C and Grilli M 2005 *Phys. Rev. Lett.* **94** 026401
- [13] de Moura F A B F, Gléria I, dos Santos I F and Lyra M L 2009 *Phys. Rev. Lett.* **103** 096401
- [14] de Moura F A B F, Vidal E J G G, Gleria I and Lyra M L 2010 *Phys. Lett. A* **374** 4152
- [15] de Moura F A B F, Caetano R A and Santos B 2012 *J. Phys.: Condens. Matter* **24** 245401
- [16] Chen D, Molina M I and Tsironis G P 1993 *J. Phys.: Condens. Matter* **5** 8689
- Pan Z, Xiong S and Gong C 1997 *Phys. Rev. E* **56** 4744
- Yamada H and Iguchi K 2010 *Adv. Condens. Matter Phys.* **2010** 380710
- [17] Kopidakis G, Komineas S, Flach S and Aubry S 2008 *Phys. Rev. Lett.* **100** 084103
- Pikovskiy A S and Shepelyansky D L 2008 *Phys. Rev. Lett.* **100** 094101
- Hajnal D and Schilling R 2008 *Phys. Rev. Lett.* **101** 124101
- Lahini Y, Avidan A, Pozzi F, Sorel M, Morandotti R, Christodoulides D N and Silberberg Y 2008 *Phys. Rev. Lett.* **100** 013906
- [18] Dias W S, Lyra M L and de Moura F A B F 2012 *Eur. Phys. J. B* **85** 7
- [19] Davydov A S 1991 *Solitons in Molecular Systems* 2nd edn (Dordrecht: Reidel)
- [20] Scott A C 1992 Davydovs soliton *Phys. Rep.* **217** 1–67
- [21] Davydov A S 1979 *Phys. Scr.* **20** 387–94
- [22] Davydov A S 1977 *J. Theor. Biol.* **66** 379–87
- [23] Davydov A S 1982 *Biology and Quantum Mechanics* (New York: Pergamon)
- [24] Brizhik L, Chetverikov A P, Ebeling W, Ropke G and Velarde M G 2012 *Phys. Rev. B* **85** 245105
- [25] Chetverikov A P, Ebeling W and Velarde M G 2011 *Physica D* **240** 1954
- [26] Hennig D, Velarde M G, Ebeling W and Chetverikov A P 2008 *Phys. Rev. E* **78** 066606
- [27] Makarov V A, Velarde M G, Chetverikov A P and Ebeling W 2006 *Phys. Rev. E* **73** 066626
- [28] Hennig D, Neissner C, Velarde M G and Ebeling W 2006 *Phys. Rev. B* **73** 024306
- [29] Hennig D, Velarde M G, Ebeling W and Chetverikov A P 2007 *Phys. Rev. E* **76** 046602
- [30] Alder B J, Runge K J and Scalettar R T 1997 *Phys. Rev. Lett.* **79** 3022
- [31] Brizhik L S and Eremko A A 1995 *Physica D* **81** 295–304
- [32] Cantu O G, Cruzeiro L, Velarde M G and Ebeling W 2011 *Eur. Phys. J. B* **80** 545–54
- [33] Velarde M G and Neissner C 2008 *Int. J. Bifurcat. Chaos* **18** 885–90
- [34] Velarde M G, Ebeling W and Chetverikov A P 2011 *Int. J. Bifurcat. Chaos* **21** 1595–600
- [35] Chetverikov A P, Ebeling W and Velarde M G 2011 *Eur. Phys. J. B* **80** 137–45
- [36] Velarde M G, Ebeling W and Chetverikov A P 2009 *Eur. Phys. J. B* **70** 217–27
- [37] Velarde M G, Ebeling W and Chetverikov A P 2005 *Int. J. Bifurcat. Chaos* **15** 245
- [38] Velarde M G 2010 *J. Comput. Appl. Math.* **233** 1432
- [39] Velarde M G, Ebeling W and Chetverikov A P 2012 *Eur. Phys. J. B* **85** 291
- [40] Ebeling W, Chetverikov A P, Röpke G and Velarde M G 2013 *Contrib. Plasma Phys.* **53** 736
- [41] Chetverikov A P, Ebeling W and Velarde M G 2013 *Eur. Phys. J.—Special Top.* **222** 2531
- [42] de Moura F A B F 2013 *Physica D* **253** 66
- [43] Astakhova T Y, Likhachev V N and Vinogradov G A 2013 *Russ. J. Phys. Chem. B* **7** 521
- [44] Likhachev V N, Astakhova T Y and Vinogradov G A 2013 *Theor. Math. Phys.* **176** 1087
- [45] Astakhova T Y, Likhachev V N and Vinogradov G A 2012 *Russ. Chem. Rev.* **81** 994
- [46] Gorodetsky A, Buzzeo M C and Barton J K 2008 *Bioconjug. Chem.* **19** 2285–96
- [47] Mallajosyula S S and Pati S K 2010 *J. Phys. Chem. Lett.* **1** 1881
- [48] Genereux C G, Boal A K and Barton J K 2010 *J. Am. Chem. Soc.* **132** 891
- [49] Cordes M and Giese B 2009 *Chem. Soc. Rev.* **38** 892
- [50] Kawai K, Kodera H, Osakada Y and Majima T 2009 *Nat. Chem.* **1** 156
- [51] Su W P, Schrieffer J R and Heeger A J 1979 *Phys. Rev. Lett.* **42** 1698
- Heeger A J, Kivelson S, Schrieffer J R and Su W-P 1988 *Rev. Mod. Phys.* **60** 781
- [52] de Moura F A B F 2011 *Int. J. M. Phys. C* **22** 63
- [53] Hairer E, Nørsett S P and Wanner G *Solving Ordinary Differential Equations I: Nonstiff Problems (Springer Series in Computational Mathematics)* (New York: Springer)

- Press W H, Flannery B P, Teukolsky S A and Wetterling W T
2007 *Numerical Recipes: The Art of Scientific Computing*
3rd edn (New York: Cambridge University Press)
- [54] de Moura F A B F 2007 *Eur. Phys. J. B* **58** 389
- [55] Sales M O and de Moura F A B F 2012 *Physica E*
45 97
- [56] Wagner M, Zart G, Vazquez-Marquez J, Viliani G,
Frizzera W, Pilla O and Montagna M 1992 *Phil. Mag. B*
65 273
- [57] Zart G S, Wagner M and Lütze A 1993 *Phys. Rev. B*
47 4108
- [58] Garnier J and Abdullaev F K H 2003 *Phys. Rev. E* **67** 026609
- [59] Fermi E, Pasta J R and Ulam S M 1955 *Los Alamos Nat. Lab.*
Report LA-1940
- [60] dos Santos C A A, Assun T F, Lyra M L and de Moura F A B F
2012 *Int. J. M. Phys. C* **23** 1240009
- [61] Katsanos D E, Evangelou S N and Xiong S J 1995
Phys. Rev. B **51** 895